Formation of Three-Dimensional Protein-Lipid Aggregates in Monolayer Films Induced by Surfactant Protein B

Silke Krol, Michaela Ross, Manfred Sieber, Stephanie Künneke, Hans-Joachim Galla, and Andreas Janshoff
Institut für Biochemie, Westfälische Wilhelms-Universität, 48149 Münster, Germany

ABSTRACT This study focuses on the structural organization of surfactant protein B (SP-B) containing lipid monolayers. The artificial system is composed of the saturated phospholipids dipalmitoylphosphatidylcholine (DPPC) and dipalmitoylphosphatidylglycerol (DPPG) in a molar ratio of 4:1 with 0.2 mol% SP-B. The different "squeeze-out" structures of SP-B were visualized by scanning probe microscopy and compared with structures formed by SP-C. Particularly, the morphology and material properties of mixed monolayers containing 0.2 mol% SP-B in a wide pressure range of 10 to 54 mN/m were investigated revealing that filamentous domain boundaries occur at intermediate surface pressure (15–30 mN/m), while disc-like protrusions prevail at elevated pressure (50–54 mN/m). In contrast, SP-C containing lipid monolayers exhibit large flat protrusions composed of stacked bilayers in the plateau region (app. 52 mN/m) of the pressure-area isotherm. By using different scanning probe techniques (lateral force microscopy, force modulation, phase imaging) it was shown that SP-B is dissolved in the liquid expanded rather than in the liquid condensed phase of the monolayer. Although artificial, the investigation of this system contributes to further understanding of the function of lung surfactant in the alveolus.

INTRODUCTION

The prerequisite for functional lung breathing is a reduced surface tension inside the alveoli, established by a material referred to as lung surfactant, which forms a thin film at the air-water interface of the alveoli comprising predominately proteins and lipids. Malfunction of this film due to the absence of particular components can give rise to serious lung diseases like alveolar proteinosis, cystic fibrosis, and silicosis. In bronchoalveolar lavage the protein content is approximately 10 wt% (Possmayer et al., 1984). Four surfactant-associated proteins have been found, two hydrophilic (SP-A and SP-D) and two hydrophobic ones (SP-B and SP-C). SP-A and SP-D play an important role in the first line defense against inhaled pathogens (Miyamura et al., 1994). Furthermore, SP-A is involved in the regulation of surfactant homeostasis (Wright et al., 1987; Rice et al., 1987; Dobbs et al., 1987; Kuroki et al., 1988), alveolar defense (Tenner et al., 1989; van Iwaarden et al., 1990), and storage and recycling of surfactant material in tubular myelin to a minor extent (Goerke, 1974; Voorhout et al., 1991). SP-A, SP-B, and phospholipids form the tubular myelin in the presence of calcium ions representing a reservoir for surfactant (Benson et al., 1984; Suzuki et al., 1989).

Surface activity of lung surfactant is dominated, however, by SP-B and SP-C. The importance of the hydrophobic fraction has been demonstrated by knockout mice and alveolar proteinosis patients. SP-B deficiency proved to be lethal for the animals (Akinbi et al., 1997), whereas results for SP-C knockout animals have not yet been reported (Hatzis et al., 1994). Congenital alveolar proteinosis with a hereditary SP-B deficiency resulted in a lack of tubular myelin (Claypool, 1988) and formation of mere SP-C precursors (Nogee et al., 1993; Vorbroker et al., 1995).

SP-B has a molecular weight of 18 kDa under nonreducing and 5 to 8 kDa under reducing conditions (Possmayer, 1988; Hawgood, 1989). Containing seven cysteines, SP-B is a homodimer, forming three intramolecular disulfide bridges and an intermolecular one. SP-B contains more polar and positively charged residues than SP-C, rendering the protein less hydrophobic (Glasser et al., 1987; Olafson et al., 1987; Curstedt et al., 1988). As revealed by circular dichroism (CD) spectroscopy, porcine SP-B adopts a predominately α-helical conformation (40–60%) with 15% contribution from β-sheet secondary structure (Cruz et al., 1995). These findings are in good agreement with the results of Vandenbussche et al. (1992), who studied the secondary structure of SP-B in a phospholipid environment. SP-B promotes a rapid insertion of phospholipids into a monolayer at the air-liquid interface and induces the formation of tubular myelin to create a reservoir for surfactant material (Cochrane and Revak, 1991; Vincent et al., 1993; Shiffer et al., 1993; Baatz et al., 1990; Yu and Possmayer, 1992). Zasadsinki and coworkers (Lipp et al., 1996, 1998; Lee et al., 1997, 1998) reported first the influence of SP-B on the phase behavior of lipid films, using fluorescence and Brewster angle microscopy in conjunction with scanning force microscopy (SFM). Recently, Lipp et al. (1998) found that at collapse pressure (>55 mN/m), SP-B containing DPPG, DPPG/POPG, or DPPC/PA/POPG films exhibit a flat monolayer coexisting with a buckled one rendering the collapse reversible and enabling the film to respread rapidly upon expansion. Both LC and LE domains are folded several micrometers into the subphase. This first-order buckling transition is thought to prevent significant loss of material into the subphase.

Received for publication 4 February 2000 and in final form 18 May 2000.
Address reprint requests to Andreas Janshoff, Institut für Biochemie, Westfälische Wilhelms-Universität, Wilhelm-Klemm-Strasse 2, 48149 Münster, Germany. Tel.: +49-251-8339765; Fax: +49-251-8333206; E-mail: janshof@nwz.uni-muenster.de.

0006-3495/00/08/904/15 $2.00

SP-C, the smallest member of the surfactant proteins, is composed of 36 amino acids with a molecular weight of 5 to 8 kDa and exhibits extraordinary hydrophobicity with an α-helix content of 70% (Possmayer, 1988; Hawgood, 1989). In most species SP-C is further modified with two palmitoyl groups covalently linked to the cysteine residues at positions 5 and 6 (Curstedt et al., 1990). It is known that SP-C and SP-B are responsible for the rapid adsorption and spreading of vesicular material from the hypophase on the monolayer until an equilibrium pressure of 50 mN/m is reached (Takahashi and Fujiwara, 1986; Oosterlaken-Dijksterhuis et al., 1991a,b). Moreover, SP-C and SP-B influence the order of phospholipids in mono- and bilayers (Pérez-Gil et al., 1992; Shiffer et al., 1993; Simatos et al., 1990; Williams et al., 1991).

Previously, we reported how SP-C is involved in the formation of a surface-associated reservoir. Wilhelmy film balance, fluorescence light microscopy (FLM), and SFM studies led to a possible scenario of how SP-C influences the morphology of phospholipid monolayers: the results suggest that SP-C induces a reversible formation of protrusions directed toward either the subphase or air, leading to fully reversible compression and expansion cycles. It was shown by means of SFM and time of flight secondary ion mass spectrometry that the protrusions formed in the plateau region of the corresponding isotherm at around 54 mN/m are composed of stacked bilayers with 5.5 to 6.5 nm layer thickness containing phospholipids and SP-C (von Nahmen et al., 1997a,b; Amrein et al., 1997; Galla et al., 1998).

In the present work, we focus on the influence of SP-B on the morphology of mixed monolayers at different surface pressures in comparison to the SP-C system, providing a scrutiny of structural changes upon compression of SP-B and SP-C containing monolayers by scanning force microscopy. SP-B displays an entirely different isotherm than SP-C, showing no plateau region at higher surface pressure. However, topographic images reveal that in analogy to SP-C, SP-B is located in the liquid expanded domains of the lipid matrix altering the phase behavior and reducing the line tension giving rise to frayed LC domains. At higher surface pressure the protein-lipid material forms three dimensional protein-rich disc-like shaped structures accompanied by a change in material properties contrast from rubber-like to a more rigid appearance. From FLM and SFM images we propose a model describing the interaction of SP-B with its lipid environment.

MATERIALS AND METHODS

Materials

SP-B (MW: 18 kDa) was isolated from porcine origin by a method described elsewhere (Curstedt et al., 1987). Human recombinant surfactant protein C (SP-C; MW: 4 kDa) was a generous gift from Byk-Gulden Pharmaceuticals (Konstanz, Germany). Both cysteine residues were palmitoylated. 1,2-Dipalmitoyl-*sn*-glycero-3-phosphocholine (DPPC) and 1,2-dipalmitoyl-*sn*-glycero-3-(phospho-rac-(1-glycerol)) (DPPG) were purchased from Avanti Polar Lipids Inc. (Alabaster, AL). 2-(4, 4-Difluoro-5-methyl-4-bora-3a, 4a-diaza-s-indacene-3-dodecanoyl)-1-hexadecanoyl-*sn*-glycero-3-phosphocholine (β-BODIPY 500/510 C_{12}-HPC, BODIPY-PC) was obtained from Molecular Probes (Eugene, OR). Solvents were high performance liquid chromatography grade and purchased from Merck (Darmstadt, Germany).

Film balance measurements

Measurements were performed on a Wilhelmy film balance (Riegler and Kirstein, Mainz, Germany) with an operational area of 144 cm^2 on pure water (18.2 M$\Omega \times$ cm, Milli-Q_{185}Plus, Millipore GmbH, Eschborn, Germany) at a temperature of 20°C. Monolayers were composed of DPPC/DPPG in a molar ratio of 4:1 with 0.4 mol% SP-C or, in the case of SP-B, with different amounts of SP-B as indicated. The lipid/protein-mixtures were spread from a chloroform/methanol solution (1:1) on the subphase. After an equilibration time of 10 min, the monolayers were compressed at a rate of 23 mm/min. With our equipment the maximum surface pressure that could be reached was about 60 mN/m.

Fluorescence measurements

Domain structures of lipid mixtures composed of DPPC and DPPG (4:1) with 0.5 mol% BODIPY-labeled PC and lipid-protein mixtures comprising DPPC/DPPG (4:1) and 0.5 mol% BODIPY-PC supplemented with 0.2 mol% SP-B were visualized by means of fluorescence microscopy (Olympus BX-FLA light microscope equipped with a *xy*-stage, Olympus, Hamburg, Germany).

Langmuir-Blodgett transfer

Langmuir-Blodgett (LB) films were prepared by spreading the lipid/protein mixture dissolved in $CHCl_3$/MeOH (1:1) on a Wilhelmy film balance (Riegler and Kirstein) with an operational area of 39 cm^2. Before spreading, a freshly cleaved mica sheet (Electron Microscopy Science, Munich, Germany) was dipped into the subphase. After an equilibration period of 10 min, the film was compressed to the desired pressure, equilibrated for another 30 min, and transferred on mica at a rate of 1.92 mm/min under constant surface pressure. LB transfers in the plateau region were performed by regulating the speed of the barrier manually (0.64 mm/min). Films with 0.2 mol% protein were transferred at 15 mN/m, 30 mN/m and 50 mN/m. It was shown by Lee et al. (1998), Leufgen et al. (1996), and Galla et al. (1998) using fluorescence microscopy, time-of-flight secondary ion mass spectrometry, and Brewster angle microscopy that structures transferred from the air-water interface onto solid substrates are essentially identical.

Additionally, for studying material properties of the monolayers we used a higher protein content of 1 mol% SP-B.

Scanning force microscopy

Surface images of the LB films were obtained at ambient conditions using a Nanoscope IIIa Dimension 3000 microscope from Digital Instruments (Santa Barbara, CA) operating in contact-, tapping-, and force modulation mode. For tapping mode, silicon NanoProbe tips (TESP, Digital Instruments) were used. The ratio of set point amplitude A_{sp} to amplitude of vibration r was set to 0.4–0.7 (moderate tapping). Contact mode/lateral force was performed using microfabricated V-shaped silicon nitride tips with a nominal spring constant of 0.06 N/m (NP, Digital Instruments). For elasticity measurements the instrument was operated in force modulation mode (FMM), which measures the local elasticity by oscillating a probe at a given frequency so that the tip indents slightly into the sample. Softer

areas cause damping of the oscillation, resulting in a lower amplitude, and are characterized by light areas in the image. Contact probes with a nominal spring constant of 0.12 N/m (Digital Instruments) were used oscillating at the resonance frequency of the bimorph piezo at 9 kHz. Tapping mode was used if not indicated otherwise.

RESULTS

Film balance measurements

Film balance experiments were performed using DPPC and DPPG in the same molar ratio (4:1) as is found in natural lung lavage for the ratio of neutral to negatively charged phospholipids (Hawgood et al., 1987). The SP-C content chosen was 0.4 mol% to be consistent with previous studies (von Nahmen et al., 1997a,b; Amrein et al., 1997; Galla et al., 1998). Because the molar ratio of SP-B to SP-C is 1:2 in natural surfactant, a SP-B dimer content of 0.2 mol% was chosen.

Pressure-area isotherms of SP-B containing monolayers (DPPC/DPPG/SP-B; Fig. 1 *C*) exhibit two small plateau regions at a surface pressure of 25–28 mN/m and at 40 mN/m. The influence of increasing amounts of SP-B on pressure-area isotherms is shown in Fig. 2 *A*. All monolayer isotherms containing more than 0.2 mol% of SP-B display the aforementioned two plateaus. The length of the first plateau at low pressure is independent of the SP-B content, whereas the second and more extended one enlarges with increasing amount of SP-B. At a surface pressure below 25 mN/m the isotherms are shifted to larger area per molecule with increasing amounts of protein. Above a pressure of 40 mN/m the isotherms of the SP-B containing monolayers are comparable to those of pure lipid films, suggesting that surfactant material has been partly squeezed out of the monolayer. Isotherms of neat SP-B monolayers also exhibit plateaus at 25 mN/m and 40 mN/m, respectively (inset, Fig. 2 *A*).

Fluidization of the lipid monolayer induced by SP-C is less pronounced than that induced by SP-B. SP-B contain-

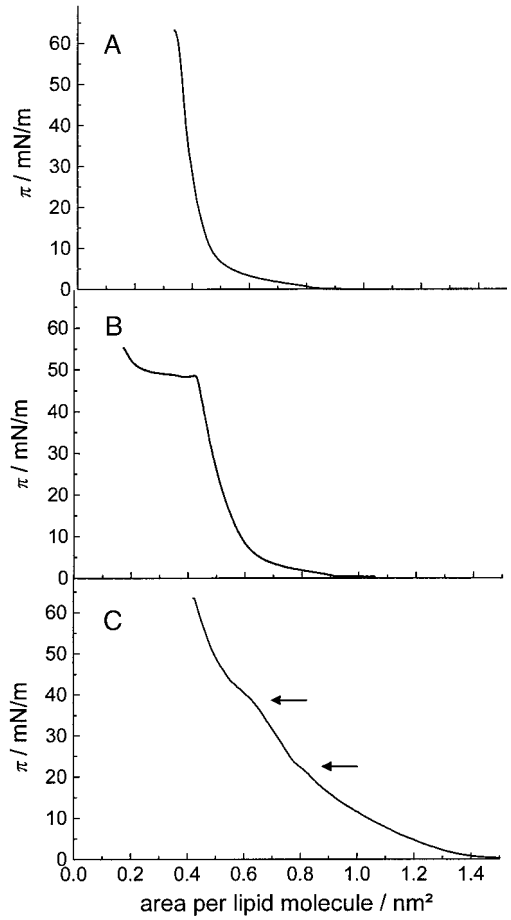

FIGURE 1 (*A*) Compression isotherm of a DPPC/DPPG monolayer in a molar ratio of 4:1. (*B*) Mixed DPPC/DPPG/SP-C (lipid molar ratio 4:1, protein content 0.4 mol%) monolayer and (*C*) DPPC/DPPG/SP-B (lipid molar ratio 4:1, protein content 0.4 mol% of the dimeric form) film at 20°C on a water subphase (pH 5.6).

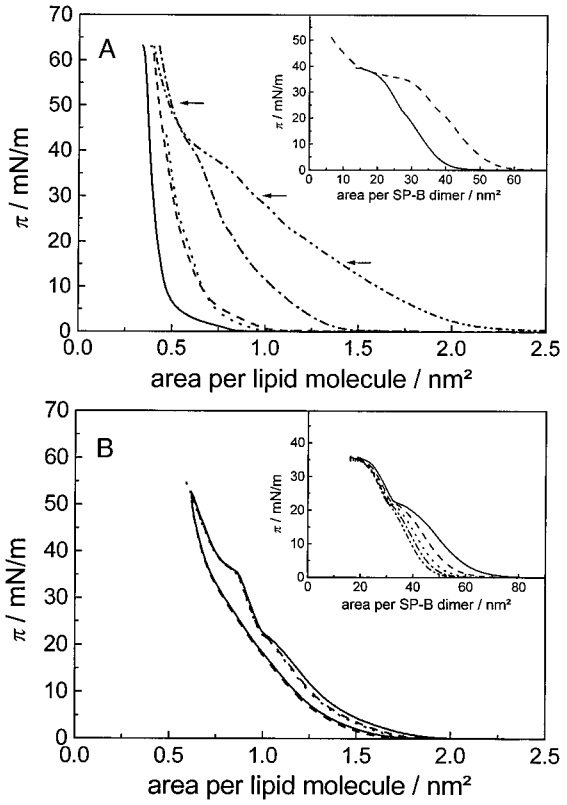

FIGURE 2 (*A*) Compression isotherms of SP-B containing monolayers with increasing amount of protein. DPPC/DPPG (lipid molar ratio 4:1) monolayer without SP-B (—), with 0.1 mol% (− −), 0.2 mol% (···), 0.4 mol% (− · −) and 1 mol% (− ·· −) on a water subphase at 20°C. The *arrows* mark the surface pressures at which the films were transferred on mica sheets for SFM. The *inset* shows compression isotherms of two neat SP-B films on a water subphase at 20°C: (—) porcine SP-B and (− −) canine SP-B, compressed to a higher pressure. (*B*) Three compression cycles of a DPPC/DPPG/SP-B (lipid molar ratio 4:1, protein content 1 mol%) monolayer indicating that no loss of surfactant material ocurs. The *inset* displays five subsequent compressions in which the area per molecule at low pressures decreases while the area per molecule is maintained for pressures >20 mN/m.

ing films display a considerably higher compressibility than monolayers containing SP-C indicating a fluidization of the lipid film by SP-B (Fig. 1, *B* and *C*). At low pressure, the isotherm of SP-C containing monolayers (Fig. 1 *B*) display the typical behavior of a lipid mixture (Fig. 1 *A*) in the absence of proteins. However, at 50 mN/m an extended plateau region occurs, giving rise to a tremendous reversible removal of lipids and peptide from the monolayer (Fig. 1 *A*). This has already been shown by von Nahmen et al. (1997a) and Post et al. (1995).

Several compression-expansion cycles of a protein-lipid film (DPPC/DPPG 4:1, protein content 1 mol%) up to a pressure of 55 mN/m did not lead to loss of material from the surface (Fig. 2 *B*). The repeated compression of a pure protein film showed a significant decrease of the length of the first plateau at 25 mN/m as well as a decrease in compressibility below this pressure (*inset*, Fig. 2 *B*). Both phenomena were due to a change in the ternary structure of the protein.

Fluorescence light microscopy

Phospholipid mixtures of DPPC/DPPG (4:1) in the absence of proteins exhibit a typical phase transition from the liquid expanded (LE) to the liquid condensed (LC) phase (Fig. 3, *A*-*C*). Compression of the film to a pressure of 5 mN/m results in the formation of dark domains of predom-

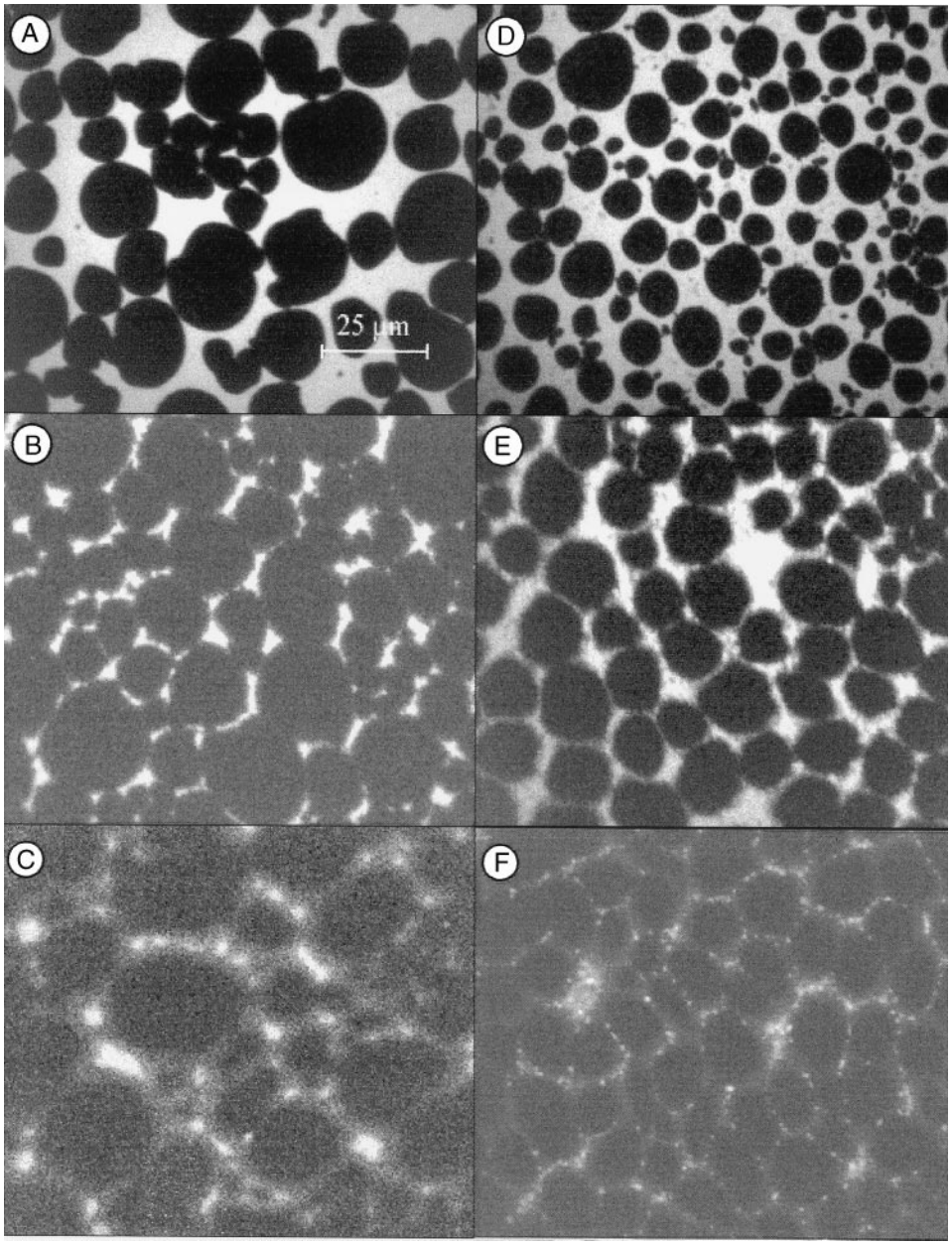

FIGURE 3 Fluorescence microscopy images of DPPC/DPPG (molar ratio 4:1) and DPPC/DPPG/SP-B (lipid ratio 4:1, protein content 0.2 mol%) films at different surface pressures with 0.5 mol% BODIPY-PC. Lipid film in the absence of protein at (*A*) 5 mN/m, (*B*) 15 mN/m, and (*C*) 50 mN/m; DPPC/DPPG/SP-B film at (*D*) 5 mN/m, (*E*) 15 mN/m, and (*F*) 50 mN/m.

inately circular shape, which continue to grow at the expense of the brighter domains (Fig. 3 *A*). While the area of the brighter phase decreases with increasing film pressure, fluorescence intensity also increases up to a pressure of 10 mN/m before it vanishes due to self-quenching of the accumulated fluorophors. At a pressure of 15 mN/m a light grey border appears around the dark domains (Fig. 3 *B*) that increases up to a pressure of 50 mN/m (Fig. 3 *C*). The influence of SP-B on the phase behavior of phospholipid monolayers composed of DPPC and DPPG with increasing pressure is shown in Fig. 3, *D–F*. The absolute area of the LE phase is considerably larger in the presence of SP-B than found for pure lipids. At elevated pressure the SP-B containing film displays particularly bright spots, indicative of strong fluorescence dye accumulation. This is in contrast to the larger bright boundaries formed by the lipid film in the absence of SP-B.

Scanning force microscopy measurements

Scanning probe microscopy offers the unique possibility of obtaining a large variety of material parameters such as topography, friction, viscoelasticity, and surface potential at high lateral resolution. However, image contrast is not always unambiguous and has to be investigated thoroughly. Here we used different techniques to unravel the influence of SP-B on monolayer morphology over a wide pressure range. Moreover, the role of SP-B versus SP-C remains to be elucidated, since it is unclear why two surface active proteins are needed for proper function of the lung. The requirements (reduction of the work of breathing, prevention of collapse of the alveoli due to differences in curvature by variation of the surface tension depending on the alveolar volume, resistance to the collapse of the surface active film, and facilitation of rapid respreading of surface active material from surface confined reservoirs) are believed to be met by adding either SP-C or SP-B to monolayers containing anionic lipids, as deduced from the work of others and our contribution (von Nahmen, 1997a,b; Lipp et al., 1998). However, little is known about the morphological details that could elucidate the dynamic function of surfactant proteins at different surface pressures. Fig. 4 *A* shows a low resolution image (30 × 30 μm) of a SP-B containing LB film (0.2 mol%) composed of DPPC/DPPG (4:1) on mica transferred at a surface pressure of 50 mN/m. A higher resolution image is included in the inset displaying the morphology of the protein-rich domains. At 50 mN/m disc-like clusters are discernable, forming a boundary of polygonal lipid-rich LC domains. Strikingly, the intersection of the stripe-like domains are enriched of these protein-induced structures. The disc-like clusters show a height of 10 ± 2 nm using tapping mode and 6–7 nm as determined by contact mode. The discrepancy between the heights obtained from tapping and contact modes can be explained by an increased compression of the structures or the occurrence of friction using contact mode, whereas tapping mode topography can be altered by differences in viscoelasticity, contact area, indentation, and adhesion. Furthermore, it is conceivable that water is incorporated in the lipid-protein clusters, giving rise to differences in height. The distribution of dark and bright pixels in the low resolution image is depicted in Fig. 4 *B*. The area taken up by the bright domains is obtained from fitting a combination of two Gaussian functions to the peak and its shoulder. The bright area occupies approximately 10% of the overall area. Fig. 5, *C–E*, Fig. 6, and Fig. 7 *A* display surface topography images of LB films composed of SP-B/DPPC/DPPG transferred to mica at different surface pressures. As already deduced from FLM images, SP-B and SP-C (von Nahmen et al., 1997a) are both dissolved in the LE phase. However, fluidization of the lipid monolayer induced by SP-B is much more pronounced than that induced by SP-C. This is further

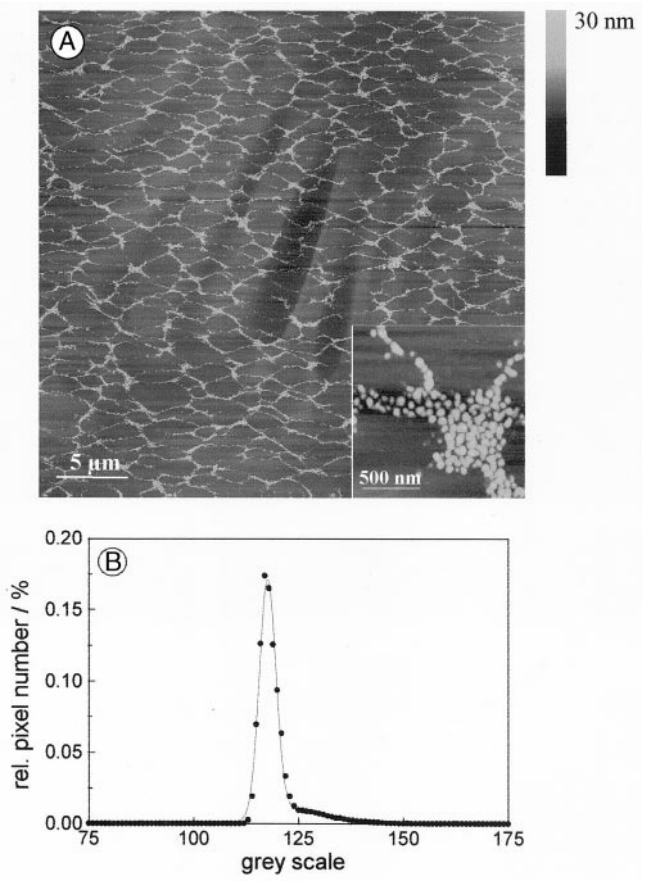

FIGURE 4 (*A*) Overview SFM image of a DPPC/DPPG/SP-B (lipid molar ratio 4:1, protein content 0.2 mol%) film on mica transferred at a surface pressure of around 50 mN/m from a water subphase at 20°C. The image size is 30 × 30 μm, the *z*-scale 30 nm. The inset shows a magnification of the disc-like structures. Image size is 1.5 × 1.5 μm. (*B*) Histogram analysis of the full scale image. The *thin solid line* represents a fit employing two Gaussian functions. The main peak represents the dark background, i.e., the condensed lipid phase; the shoulder marks the light disc-like domains.

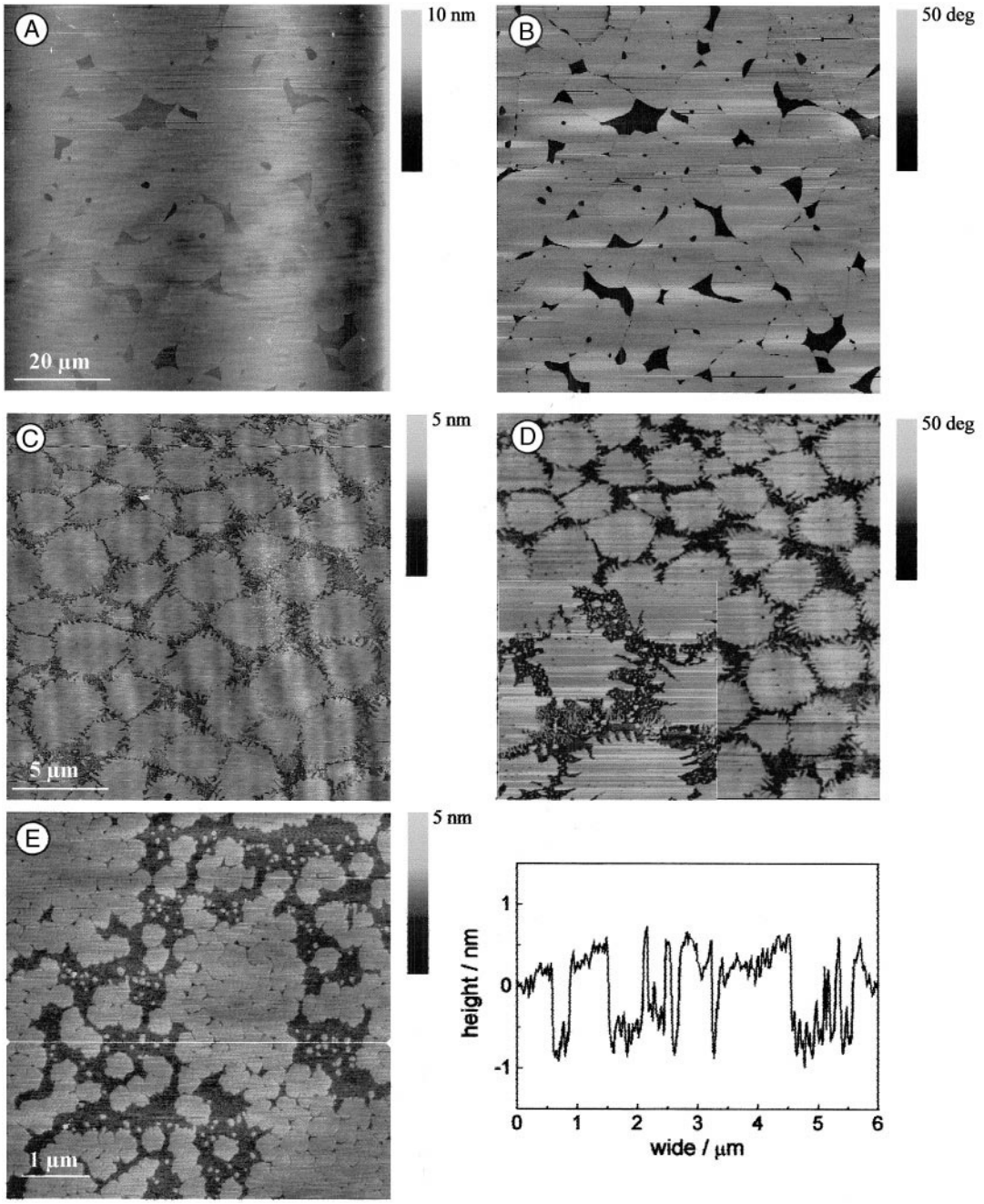

FIGURE 5 (*A*) SFM image (topography) and (*B*) phase image of a DPPC/DPPG (4:1) monolayer transferred onto mica at 15 mN/m. (*C*) SFM image (topography) and (*D*) phase image of SP-B containing phospholipid films (DPPC/DPPG in a molar ratio 4:1, protein content 0.2 mol%) transferred at 15 mN/m. The *inset* in (*D*) shows a magnification of the LE phase. The image size is 4.6 × 4.6 μm, and the *z*-scale is 54 degrees. (*E*) SFM image (contact mode) of a SP-B containing phospholipid film at slightly lower surface pressure (~10 mN/m) showing small polygonal LC domains assembling to larger LC domains. The line scan exhibits the same height difference of the LC and LE phase as observed for the DPPC/DPPG film (data not shown).

supported by comparing the areas occupied by the protein-rich domains of monolayers with 0.2 mol% (Fig. 6) and 1 mol% SP-B (Fig. 8).

At 15 mN/m (Fig. 5 *C–E*) two phases (LE and LC) are discernible, exhibiting contrast in phase imaging and topography. The LC phase is approximately 1 nm higher than the LE phase, as indicated by the line scan next to the image (Fig. 5 *E*). The higher and stiffer domains (LC), as determined by tapping mode and force modulation, show a polygonal shape in which the prevailing structures exhibit a diameter of about 100 nm, although smaller domains with diameters <10 nm are also observable. The polygonal do-

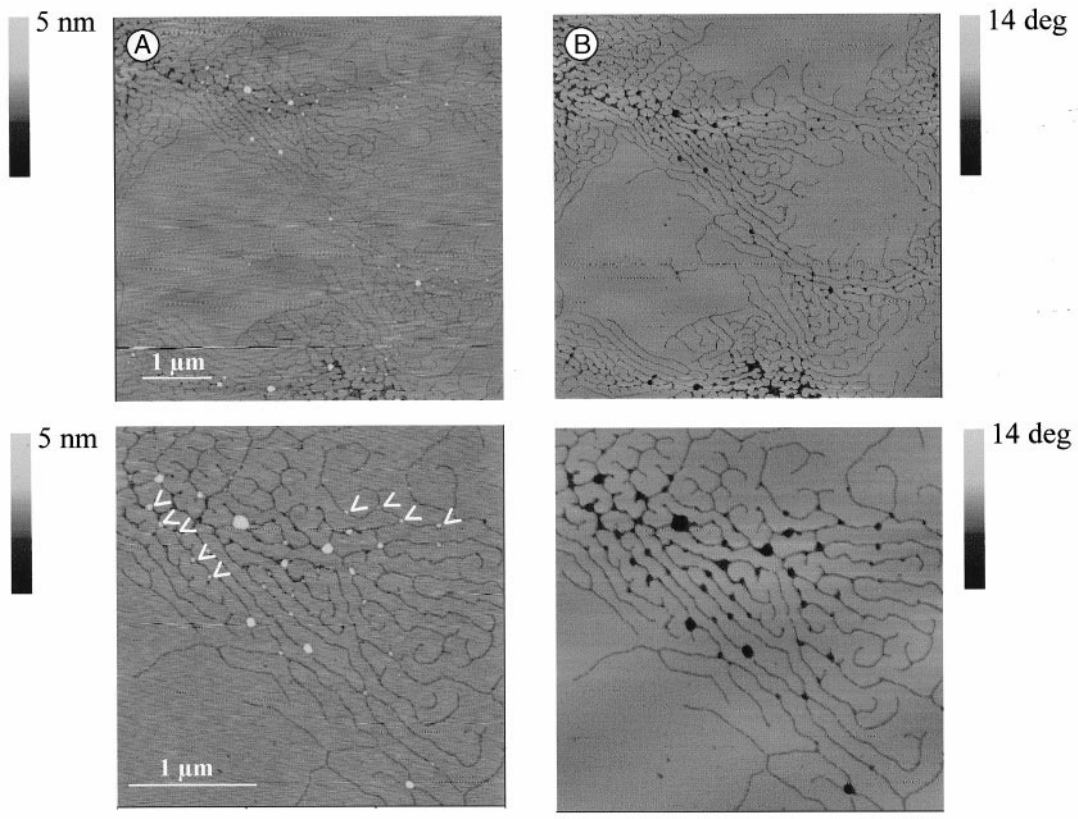

FIGURE 6 (*A*) SFM image (topography) and (*B*) phase image of SP-B containing phospholipid films (DPPC/DPPG in a molar ratio 4:1, protein content 0.2 mol%) transferred at 30 mN/m. The *arrows* label the disc-like protrusions forming at intersections of the line-shaped domains of the protein rich LE phase. The phase image displays strong contrast, in which the darker phase indicates low elasticity or high viscous losses at tip-sample contact and the brighter phase stiffer material with low energy dissipation.

mains assemble into larger structures of several micrometers, still maintaining spaces as thin lines of LE phase between them (Fig. 5 *E*). In contrast to the polygonal structure of the domains with SP-B, pure DPPC/DPPG (4:1) monolayers (Fig. 5, *A* and *B*) transferred onto mica at a pressure of 15 mN/m show larger, circular LC domains ($>$20 μm in diameter).

At a surface pressure of 30 mN/m, the LE phase is still present, showing a filamentous boundary of mostly suppressed height (1 nm) and low phase shift (Fig. 6). However, the occurrence of small protrusions of various heights exceeding those of the LC domains should be pointed out. Sometimes we also observed a slightly higher LE phase. This could be due to small deviations in surface pressure during transfer of the film. Globular structures are formed solely from the LE phase. Slight differences in surface pressure due to inhomogeneous film transfer result in a variation of the dimensions and number of the protrusions. Generally, the LC domains show a hexagonal or rhombus-like structure with a mean diameter of 330 to 430 nm. Higher protein content increases the number of LC domains but reduces their size. The small protrusions occur almost equidistant at a distance of 200 to 300 nm (marked with arrows in Fig. 6).

SFM images of LB-films transferred at around 50 mN/m display a typical phase separation represented by lower homogenous domains which are surrounded by disc-like structures with an average diameter of 55 $\pm$ 10 nm and a height of 10 $\pm$ 2 nm, reminiscent of a string of pearls (Fig. 7 *A*). The crossing points of the string-like domains are characterized by an increased occurrence of the disc-like clusters. The diameter of the enclosed LC domains, presumably composed of DPPC and DPPG, is in the range of 3 to 10 μm. The size of the rhomboidal LC domains depends on the applied surface pressure. A film compressed to a pressure of nearly 50 mN/m, followed by an equilibration at 50 mN/m, shows smaller LC domains than one that is compressed to a pressure of only 52 mN/m and then equilibrated at 50 mN/m.

SP-C containing monolayers transferred in the plateau region at around 50 mN/m have been previously described in great detail (von Nahmen et al., 1997b; Amrein et al., 1997; Galla et al., 1998). The occurrence of large, flattened and smooth protrusions composed of stacked lipid bilayers dominate the picture (Fig. 7 *B*). The step height of the

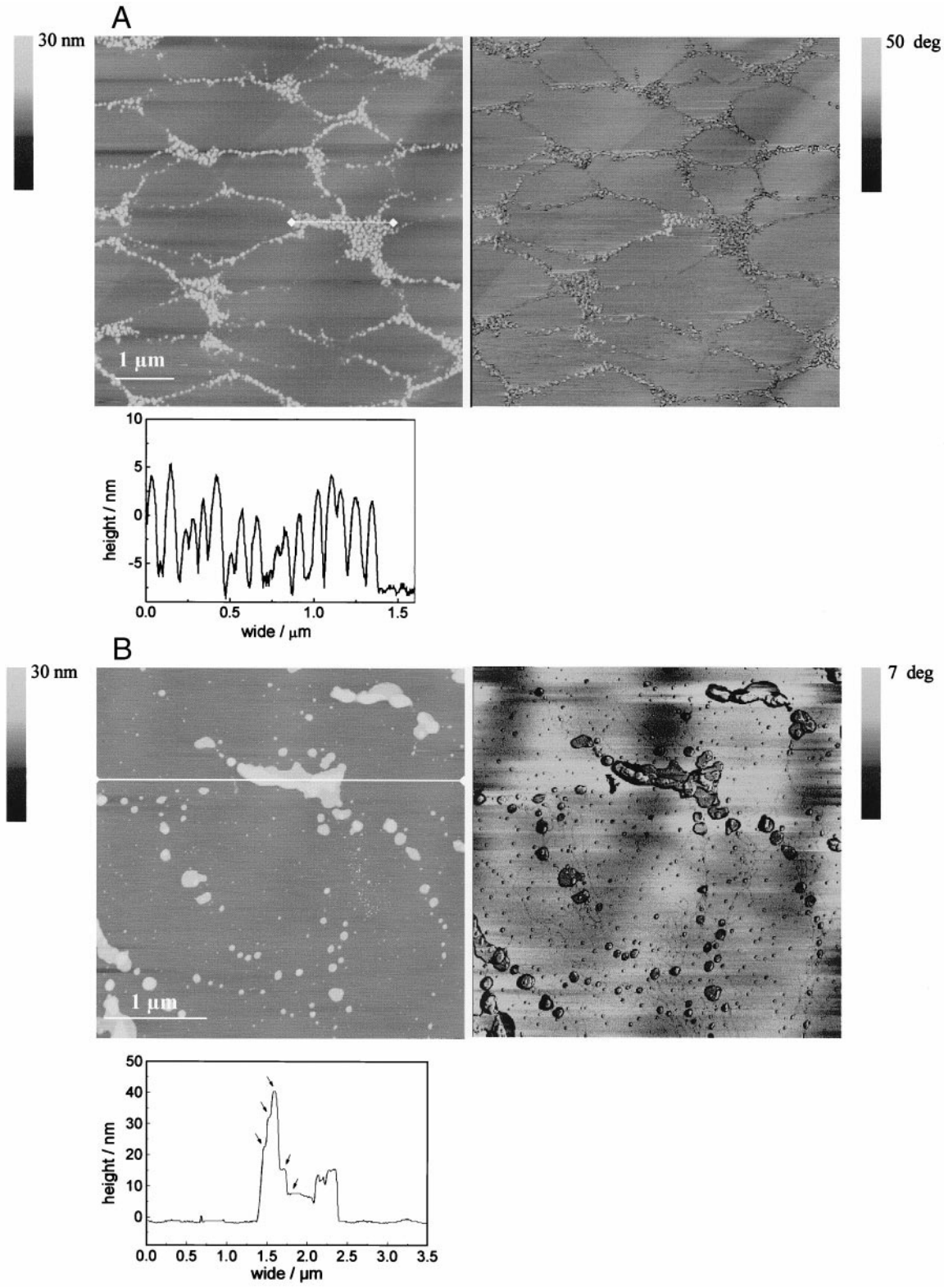

FIGURE 7 Comparison between topography and phase image of (*A*) SP-B and (*B*) SP-C containing films (DPPC/DPPG 4:1, protein content 0.2 mol% for SP-B and 0.4 mol% for SP-C) transferred at 50 mN/m (SP-B) and 54 mN/m (SP-C) onto mica. SP-B forms disc-like protrusions of one bilayer thickness, whereas SP-C tends to form extended plateaus consisting of stacked bilayers (height steps labeled by *arrows*).

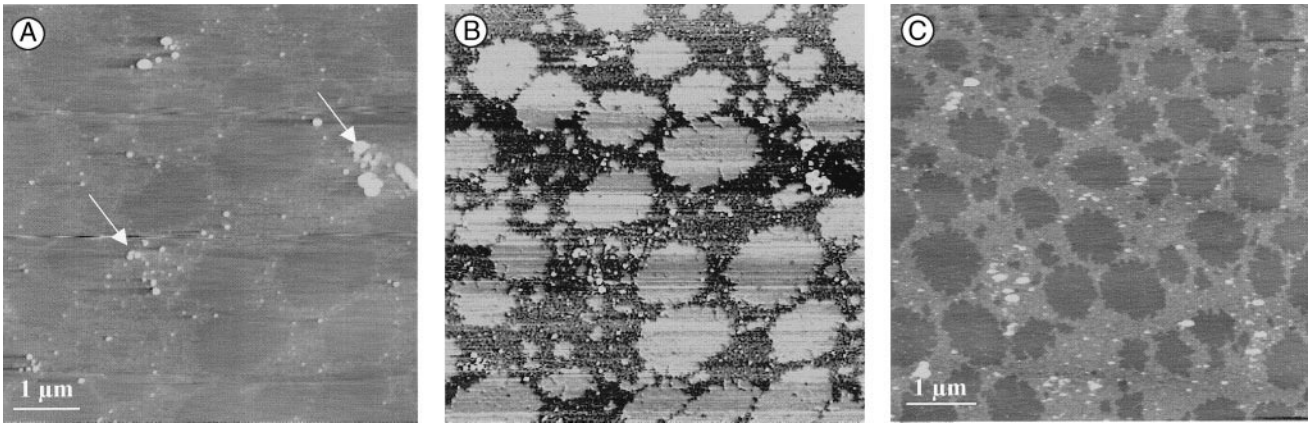

FIGURE 8 Material properties contrast of a SP-B containing LB film transferred at 30 mN/m (DPPC/DPPG 4:1, protein content 1 mol%). The higher protein content results in an increased area of the protein-enriched LE phase. The size of the LC domains is decreased. (*A*) Topography image obtained from tapping mode (*z*-scale: 15 nm), *arrows* mark the protrusions (*B*) corresponding phase image (*z*-scale: 15 degrees). The darker areas represent softer material or viscous losses; the lighter ones correspond to the LC domains exhibiting a higher Young modulus. (*C*) SFM image obtained from self-excitation mode imaging in the overall attractive regime, rendering the sample less damaged (*z*-scale: 15 nm). Size of all images is 6 × 6 μm.

patches is 6.5 ± 0.5 nm determined by contact mode at 200 pN load force and 7.5 ± 0.5 nm determined by tapping mode (this study). Occasionally the bilayer structures exceed 5 to 10 μm in diameter (data not shown). These findings are supported by FLM (von Nahmen et al., 1997a,b) at the air-water interface showing that lipid-dye (NBD-PC) is dissolved in the same part of the film (LE phase) as the protein. This was demonstrated by using fluorescently labeled protein. Lee et al. (1998) could prove the same for SP-B containing monolayers using FLM and polarized FLM.

Material properties contrast

A higher content of SP-B decreases the average domain size of the LC phase, whereas it increases the area occupied by the protein-rich LE phase. LFM, FMM, and phase imaging reveal that the protein-rich phase exhibits different viscoelastic properties, friction coefficients, or adhesion between tip and sample than the lipid-rich phase (Fig. 8). As pointed out by others, the extraction of quantitative or even qualitative data from images produced by FMM and phase imaging is rather cumbersome and depends strongly on the experimental conditions (Jourdan et al., 1999; Gotsmann et al., 1999).

Fig. 8 shows images of a SP-B containing monolayer of DPPC/DPPG (4:1) with 1 mol% of protein transferred onto mica at a pressure of 30 mN/m employing moderate tapping conditions (r = 0.5). Although the topography contrast (Fig. 8 *A*) shows that the protein-rich domains are higher and more corrugated than the smooth LC domains, the phase image displays contrast inversion due to differences in viscoelasticity of the LC domains in comparison to the protein-enriched phase (Fig. 8 *B*). Furthermore, a pronounced texture of the soft domains can be observed in the phase image that provides high contrast. The occurrence of globular protrusions is also visible (*arrows*). In particular, the disc-like structures originating from the soft LE phases at 30 mN/m exhibit a very low phase shift (very dark circular areas). This could be due to the viscous properties of the material giving rise to an additional energy loss of the cantilever oscillation. Fig. 8 *C* shows an image employing the self-excitation mode using a special quality enhancement circuit (Q-control) developed by Anczykowski et al. (1998). The self-excitation mode enables one to image with extremely low load in the overall attractive regime, resulting in an enhanced resolution of the soft domains due to less damaging of the sample and reduced indentation. Energy loss is also reduced considerably. The images obtained from tapping and non-contact mode are basically identical, indicating that destruction of the sample can be neglected. In order to support our findings on material properties contrast produced by protein insertion, we used FMM as supplied by Digital Instruments using the same LB film (Chi et al., 1998) (Fig. 9). We found that the LC domains represent a stiffer material with higher Young modulus than the protein-enriched LE phase. It should be pointed out that FMM can produce controversial results depending on the frequency (Jourdan et al., 1999). However, all findings from scanning force microscopy aim in the same direction, confirming the result obtained from FLM. The globular protrusions exhibit an extremely soft nature in the pressure regime up to 30 mN/m. At higher surface pressure the structure shows a higher phase shift similar to the protrusions induced by SP-C, leading to the hypothesis that the excluded material might be of similar nature. Both SP-C and SP-B containing monolayers transferred to mica at a pressure of >50 mN/m show protrusions that exhibit typical edge effects in the phase image, probably due to topography and differences in contact area between tip and sample. However, changes in stiffness are not as pronounced as those observed

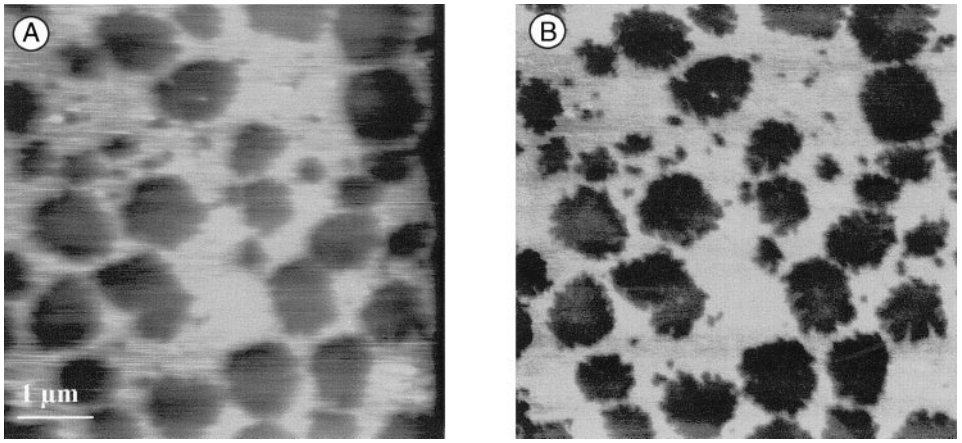

FIGURE 9 Force modulation mode image of a SP-B containing LB film transferred at 30 mN/m (DPPC/DPPG 4:1, protein content 1 mol%). (*A*) Topography (*z*-scale: 25 nm). (*B*) Amplitude (*z*-scale: 2 nm). The light phase indicates material with low elastic modulus; the dark areas represent the LC phase exhibit a higher elastic modulus. Image sizes, 6 × 6 μm.

at a film pressure of <30 mN/m. The protrusions seem to display the same Young modulus as the monolayer.

Lateral force microscopy was used in order to find contrast based on different tip-sample interactions. Fig. 10 shows topography forward and backward traces. The protein-containing phase displays the strongest interaction with the tip, resulting in a bright appearance in the forward scan and reverted contrast in the backward scan direction. Contrast inversion of that kind provides reasonable evidence that the observed contrast is due to differences in friction rather than to lateral forces arising from changes in topography. The lateral force consists of two components, one based on tribology and one on topography. Only the tribology term depends on the scan direction. If the contrast is independent of the scanning direction, assuming a scan angle of 90 degrees, it is merely topography, which causes torsion of the cantilever. Therefore, contrast inversion provides a qualitative measure for the origin of lateral forces. Again, the texture of the soft phase is well displayed by LFM contrast. In addition, the light spots in topography referred to as the disc-like protrusions generate high contrast in LFM mode, which is not due to topography evident from the contrast inversion of forward and backward scan direction, but apparently is caused by strong tip-sample interaction, indicating a higher friction coefficient of the protein-rich phase (Fig. 10, *B* and *C*).

The interpretation of phase image contrast in tapping mode is complicated, largely because the tip-sample force is a nonlinear function of the distance. Assuming that the vibration of the cantilever is harmonic, and the force constant changes and the frequency shift are small compared to ω and k, respectively, the phase angle shift $\Delta\Phi$ is expressed as

$$\Delta\Phi \approx 2Q_{\text{eff}}\frac{\Delta\omega}{\omega_0} \tag{1}$$

Q_{eff} denotes the effective quality factor of the vibrating cantilever. Magnov et al. (1997) pointed out that a qualitative interpretation of the phase contrast can be based on the assumption that the change of the phase angle is roughly proportional to the time average of the stiffness of the LB film, which is, following the Hertz model, a product of the

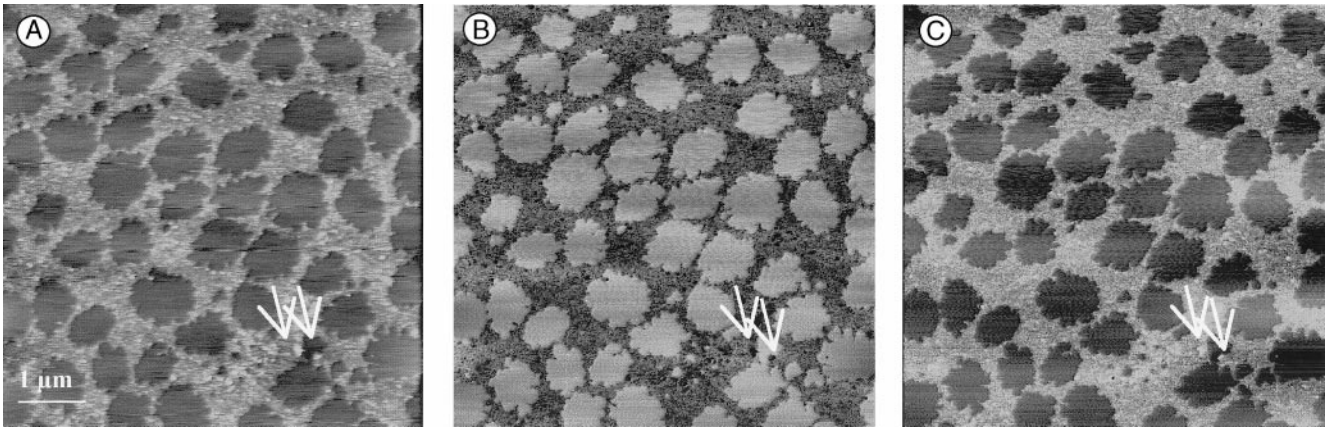

FIGURE 10 Lateral force microscopy images of a SP-B containing LB film transferred at 30 mN/m (DPPC/DPPG 4:1, protein content 1 mol%). The disc-like protrusions are marked with *arrows*. (*A*) Topography (z-scale: 25 nm). (*B*) and (*C*) Lateral force images in the (*B*) backward and (*C*) forward scan directions (*z*-scale: 0.3 V). Image size, 6 × 6 μm.

contact radius and the Young modulus. Therefore, depending on the ratio $r = A_{sp}/A_0$, the amplitude chosen by the set point A_{sp} and the driving amplitude A_0 the contrast can be due to differences in the elastic moduli or the contact area producing reverse contrast. Magnov et al. found that r ratios of 0.4 to 0.7, referred to as moderate tapping, generally produce contrast based on differences in elasticity. Hard tapping, $r < 0.3$, leads to a considerable contribution of indentation; therefore, contrast is based on differences in contact area between tip and sample, which increases with decreasing Young modulus. As a consequence, the soft material appears lighter under hard tapping conditions, whereas the phase shift is smaller on soft material at moderate tapping. However, the driving amplitude needs to be large enough to ensure that the probe is not captured by the surface contamination layer.

However, Anczykowski et al. (1999) found that energy dissipation plays the pivotal role in the formation of phase contrast. Without specifying the kind of tip-sample interaction force, the mean power dissipation at $\omega = \omega_{res}$ is solely responsible for the observed phase contrast. Both phase shift and energy dissipation increase with decreasing tip-sample distance. It can be shown that $\Delta\Phi$ is larger on surfaces with low energy dissipation, accounting for the observed contrast. Darker areas represent high energy dissipation from viscous origin; bright areas are regions of low dissipation.

Although the origin of phase contrast is discussed controversially and suitable quantification protocols remain to be developed, phase imaging is a sensitive tool to detect differences in viscoelasticity.

DISCUSSION

Analysis of lung lavage revealed that pulmonary surfactant consists mainly of lipids such as dipalmitoylphosphatidylcholine and phosphatidylglycerols besides other unsaturated phospholipids, fatty acids, cholesterol, and proteins. Due to their amphiphilic nature, SP-B and SP-C play a pivotal role in determining the surface properties of lung surfactant. In order to mimic the natural situation of alveolar air-liquid interface we used the air-water interface as provided by a film balance setup. From the large variety of compounds we have chosen two different systems, a phospholipid mixture consisting of DPPC and DPPG in a molar ratio of 4:1 supplemented with either SP-C (0.4 mol%) or SP-B (0.2 mol%) as found in native lung surfactant. From previous measurements on SP-C containing Langmuir monolayers, we are able to postulate a model for the biophysical role of SP-C in pulmonary surfactant (Scheme 1).

Fluorescence microscopy in conjunction with SFM reveals that upon compression of the monolayer representing the exhalation situation, surface-confined reservoirs are induced by SP-C. It was shown that these protrusions are due to a stacking of bilayers folded from the monolayer at elevated pressure. FLM and time of flight secondary ion mass spectrometry images clearly show that the protrusions originate exclusively from the protein-enriched domains, the former LE phase of the low surface pressure region of the isotherm (Galla et al., 1998).

Zasadzinski and coworkers (Lipp et al., 1997; Lee et al., 1998) recently provided an extensive study on SP-B containing lipid monolayers based on fluorescence microscopy, Brewster angle microscopy, and polarized fluorescence microscopy at the air-water interface as well as the air-solid interface. This system was composed of palmitic acid (PA) containing various amounts of SP-B ranging from 5 to 20% per weight. Lipp et al. (1998) studied the influence of SP-B on the collapse mechanism of anionic lipid mixtures. They found that a first-order transition from a flat monolayer to a buckled one occurs, which presumably explains how the lung surfactant copes with low surface tension.

Taneva and Keough (1994) already predicted that the proteins have to be squeezed out of the monolayer surrounded by merely a few phospholipid molecules based on film balance measurements and calculations of the mean area per residue. Pastrana-Rios et al. (1995) reconstituted a monolayer film at the air-water interface containing DPPC and one of the hydrophobic surfactant proteins. Using external reflection absorption infrared spectroscopy, they found a loss of SP-B from the monolayer above a surface pressure of 40 mN/m, which was irreversible for a DPPC-containing film but reversible in the case of POPG/DPPC (Pastrana-Rios et al., 1994).

In contrast to the results of Taneva et al. (1994) reporting a kink at a pressure of 40 mN/m with a protein content higher than 0.5 mol%, we already find an effect of SP-B on the phase transition of lipid monolayers at lower protein concentrations (0.2 mol%) characterized by a plateau at lower pressure. From comparison of isotherms obtained from pure SP-B and the lipid mixture in the absence of protein, we presume that a phase separation of a lipid-enriched and protein-enriched phase occurs. At a surface pressure above 40 mN/m the isotherm shows nearly the compressibility of the pure lipid mixture. The findings are consistent with SP-B/lipid aggregates squeezed out of the monolayer into a third dimension.

As far as the neat SP-B monolayer is concerned, we observed a significant change in compressibility and area per molecule between the first and the second compression cycles. We propose that an irreversible change of the protein's ternary structure might occur at the first compression, rendering the film less compressible at the second compression. Furthermore, we observed a decrease in length of the first plateau region along with additional compression/expansion cycles, supporting the hypothesis of an irreversible change in ternary structure (Fig. 2, *B* and *inset*, pure SP-B).

Fluorescence microscopy reveals that the proteins are most likely located in the liquid-expanded phase. Fluorescent-labeled DPPC is dissolved in the LE phase and is, therefore, a measure of domain size. Increasing the amount

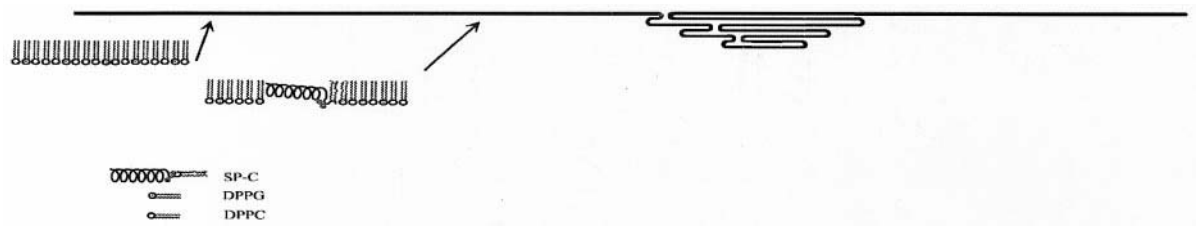

Scheme 1. Proposed model for the observed squeeze out of material supported by lung surfactant protein C (Galla et al., 1998).

of protein results in an increase of the former LE phase and a decrease of the LC domain size, indicating that the protein fluidizes the monolayer. This is in agreement with the results obtained by Lee et al. (1997) confirming that SP-B is dissolved in the fluid phase of the lipid monolayer detected by using both a fluorescently labeled protein and a labeled lipid assigning the fluid phase.

SFM has contributed significant information about topography and tribology of LB films. In particular, previous studies dealing with the biological role of SP-C as a surface-active component of pulmonary lung surfactant demonstrated the importance of SFM to provide valuable information about the formation of surface-confined reservoirs induced by SP-C. Amrein et al. (1997) demonstrated that, indeed, the discrete steps observed by contact mode SFM arise from protein containing phospholipid bilayers folding like a sheet of paper into the third dimension. These findings basically explain the observation in fluorescence microscopy and surface pressure-area isotherms, i.e., the fluorescence intensity profile indicating protrusions consisting of discrete layers (von Nahmen et al., 1997) as well as the reversible compression/expansion cycles (Post et al., 1995).

The morphology of SP-B containing phospholipid films is different from that of SP-C. Instead of forming extended sheets of bilayers homogeneously stacked on top of each other, distributed disc-like clusters exhibiting an average diameter of 55 $\pm$ 10 nm and an approximate height of 10 $\pm$ 2 nm are observed. The findings can be explained in terms of a low cooperativity formation of protein protrusions involving only a limited amount of lipids. Formation of regular disc-like structures at elevated surface pressure was also reported by Lipp et al. (1998) using DPPG and SP-B at 37°C on a saline subphase. These results support the assumption that independent of the conditions, SP-B forms nearly the same kind of structure at high surface pressure, thus suggesting a universal mechanism for the interaction with saturated anionic lipids.

Scheme 2 shows the proposed model based on our results and those described by others (Taneva et al., 1994; Pastrana-Rios et al., 1995; Oosterlaken-Dijksterhuis et al., 1991a,b; Williams et al., 1991). SP-B is represented by two helical parts exhibiting a charge and hydrophobicity gradient enabling the molecule to interact with negatively charged phospholipid headgroups and the core of the membrane. Helical wheel projection based on the secondary structure found by Cruz et al. (1995) for porcine SP-B dimers reveal an excess of positive charges on the one side of the three helices and the cysteine residues on the other side, which are responsible for the formation of disulfide bridges with the fourth helix (Anderson et al., 1995). Furthermore, helical wheel projection displays the results of Cruz et al. (1995) who found that the aromatic tryptophan residue is directed to the outside of the dimer, whereas the second aromatic tyrosin points to the other dimer (Scheme 2 *A*). Interaction of the charged SP-B helices with negatively charged phospholipids presumably induces a phase separation between charged and uncharged lipids. The peptide helices are capable of shifting against each other in order to compensate for the increasing surface pressure by small changes in ternary structure. This is possible for either neat protein films or mixed monolayers, supporting our assumption. In a lipid environment, ordering processes of negatively charged PG induced by SP-B have been described for bilayer systems (Baatz et al., 1990; Creuwels et al., 1996; Pérez-Gil et al., 1995). However, no change in acyl chain conformation of the lipids was found within the membrane interior (Baatz et. al., 1990, Vandenbussche et al., 1992).

Scheme 2 *B* envisions a possible scenario of domain formation as observed in our study. It is assumed that the SP-B dimer is attached to the headgroups of surrounding PG molecules via electrostatic interaction, giving rise to an immobilization of a certain amount of lipids. A pressure-induced change in conformation of the protein, which remains to be elucidated, is the initial starting point of the squeeze-out process.

Assuming an area of 2378 Å^2 for a single SP-B dimer and 43 Å^2 for the area of phospholipids as deduced from pressure-area isotherms at a pressure of 30 mN/m, we calculated that the protein in a phospholipid monolayer containing 0.2 mol% SP-B occupies 10% of the total area. Histogram analysis of SFM images (Fig. 4 *B*) provides a ratio of light to dark areas of 1:10, in good agreement with our calculations based on pressure-area isotherms. Thus, the diameter of a single protein can be determined to be 49 Å compared to 6.5 Å for a lipid. Pérez-Gil et al. (1995) and Shiffer et al. (1993) found that monomeric SP-B is associated with approximately 50 lipids. The roughly circular protrusions exhibit a lipid to SP-B dimer ratio of approximately 260:1, calculated by assuming a mean diameter of the disc-like

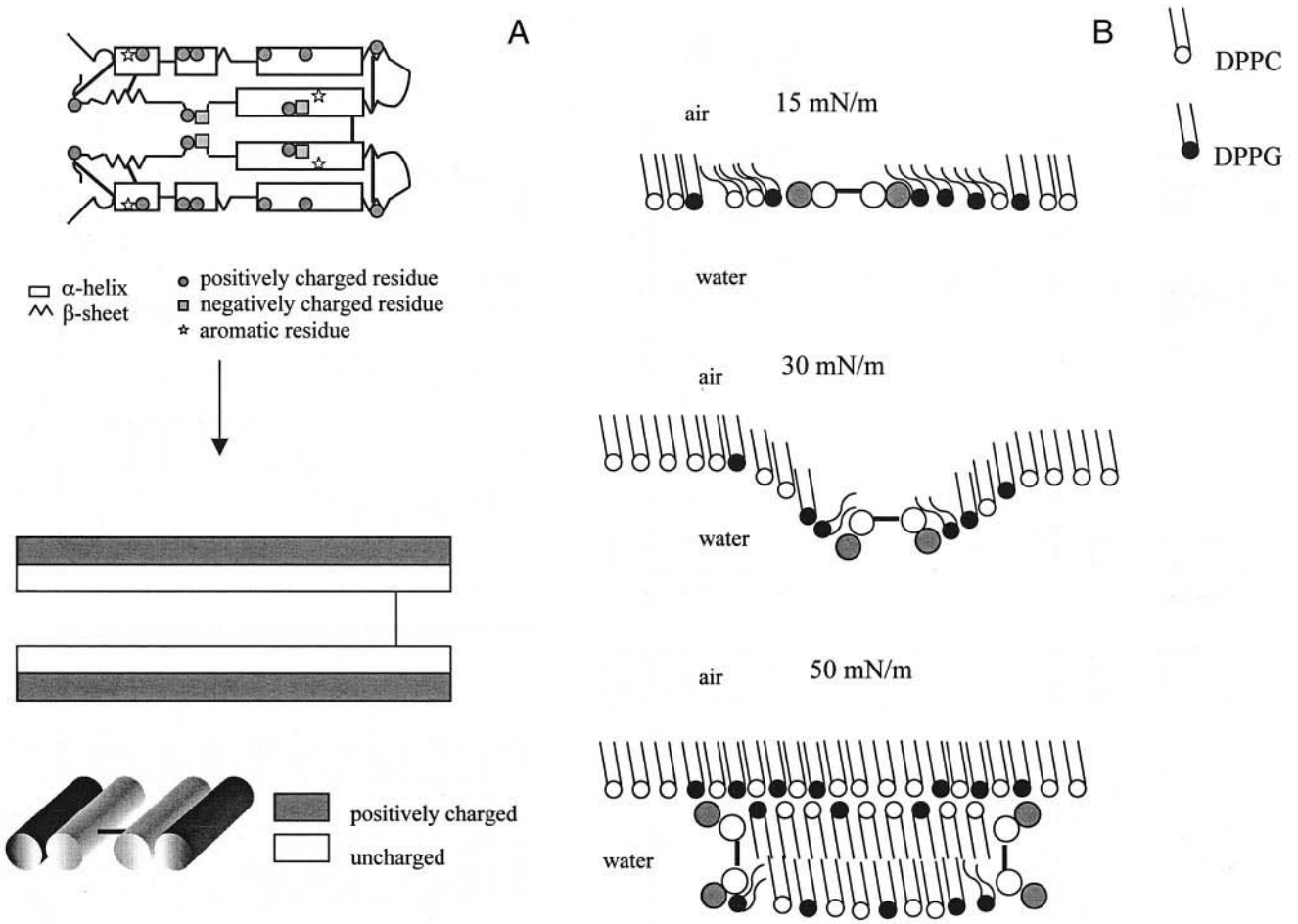

Scheme 2. New model describing the formation of disc-like protrusions of SP-B containing phospholipid films. (*A*) Proposed protein structure with two different charged helices per monomer (Cruz et al., 1995). (*B*) Possible explanation for the mechanistic role of SP-B in a lipid monolayer during compression.

protrusions of 65 nm, an area per molecule of 0.4 nm^2 for the lipid molecules, and a lateral extension of approximately 3.3 nm for the protein. In principle, the proposed model presumes that the protruded discs consist of phospholipid bilayers surrounded by a rim of proteins reducing the line tension.

At a surface pressure above 40 mN/m, loss of proteins from the monolayer occurs (Taneva et al., 1994; Pastrana-Rios et al., 1995). Furthermore, Pastrana-Rios et al. (1995) reported an irreversible loss depending on the protein concentration in the monolayer. A possible explanation would be the formation of protrusions as depicted in Scheme 2 *B* consisting of bilayers stabilized by SP-B molecules at the edges. Compression of the monolayer results in a storage of monolayer material in a bilayer pocket adjacent to the monolayer phase. Irreversible loss is conceivable at elevated pressure by formation of soluble bilayer satellites. It is possible that these SP-B stabilized bilayer fragments are identical to the disc-like structures observed by Williams et al. (1991) for systems containing DPPC/DPPG and SP-B. SP-B could function like a zipper, enabling disc-like bilayers to squeeze rapidly out of the monolayer and respread during the breathing cycle, exchanging surfactant material with tubular myelin.

CONCLUSIONS

Based on our findings and in agreement with other studies (Lipp et al., 1996; Lee et al., 1998) SP-B was found to fluidize lipid monolayers. It reduces the domain size of the condensed phase while it stabilizes the film by moving the collapse to higher surface pressure. Due to reduction of the LC domain size, SP-B renders the collapse more reversible since each domain collapses independently, which facilitates respreading of material in the monolayer upon expansion. Remarkably, the protein-rich phase is maintained even at elevated surface pressure. As deduced from the phase images obtained from SP-B containing LB films and transferred at 30 mN/m on the substrate, the line tension of the condensed domains is strongly reduced by the influence of

the protein, resulting in a tremendous increase of the interface between fluid and solid phases due to electrostatic repulsion. In comparison to the SP-C containing system, protrusions are limited in size and exhibit a globular or disc-like structure of uniform height (8–10 nm). Presumably the protrusions are bilayer patches composed mainly of peptide and anionic lipids. Smaller protrusions permit faster response to changes in surface pressure, therefore rendering the system prepared for a dynamic response.

The authors gratefully acknowledge the outstanding collaboration with Harald Fuchs and his group, who provided us with equipment and fruitful discussions on scanning probe microscopy. We also thank Boris Ancyzkowski for his valuable input and discussions on tapping mode SFM. Bovine SP-B was a generous gift from Lambert Creuwels and Lambert van Golde (Utrecht, The Netherlands). Human recombinant surfactant protein C (SP-C) was provided from Byk-Gulden Pharmaceuticals (Konstanz, Germany). Financial support by the Deutsche Forschungsgemeinschaft (SI 670/1–1 and SFB 424) is gratefully acknowledged. Andreas Janshoff is a recipient of a habilitation fellowship granted by the DFG (JA 963/1–1).

REFERENCES

Akinbi, H. T., J. S. Breslin, M. Ikegami, H. S. Iwamoto, J. C. Clark, J. A. Whitsett, A. H. Jobe, and T. E. Weaver. 1997. Rescue of SP-B knockout mice with a truncated SP-B proprotein: function of the C-terminal propeptide. *J. Biol. Chem.* 272:9640–9647.

Amrein, M., A. von Nahmen, and M. Sieber. 1997. A scanning force- and fluorescence light microscopy study of the structure and function of a model pulmonary surfactant. *Eur. Biophys. J.* 26:349–357.

Anczykowski, B., B. Gotsmann, J. P. Cleveland, H. Fuchs, and V. B. Elings. 1999. How to measure energy dissipation in dynamic force microscopy. *Appl. Surf. Sci.* 140:376–382.

Anczykowski, B., J. P. Cleveland, D. Krüger, V. Elings, and H. Fuchs. 1998. Analysis of the interaction mechanisms in dynamic mode SFM by means of experimental data and computer simulation. *Appl. Phys. A.* 66:S885–S889.

Anderson, M., T. Curstedt, H. Jörnvall, and J. Johansson. 1995. An amphipathic helical motif common to tumourolytic polypeptide NK-lysin and pulmonary surfactant polypeptide SP-B. *FEBS Lett.* 362: 328–332.

Baatz, J. E., B. Elledge, and J. A. Whittsett. 1990. Surfactant protein SP-B induces ordering at the surface of model membrane bilayers. *Biochemistry.* 29:6714–6720.

Benson, B. J., M. C. Williams, K. Sueishi, J. Goerke, and T. Sargeant. 1984. Role of calcium ions in the structure and function of pulmonary surfactant. *Biochim. Biophys. Acta.* 793:18–27.

Chi, L. F., M. Gleiche, and H. Fuchs. 1998. Study of long-range tilt orientation in fatty acid monolayers by dynamic scanning force microscopy. *Langmuir.* 14:875–879.

Claypool, W. D. 1988. Pulmonary alveolar proteinosis. *In* Pulmonary Diseases and Disorders. A. P. Fishman, editor. McGraw-Hill, New York.893–900.

Cochrane, C. G., and S. D. Revak. 1991. Pulmonary surfactant protein B (SP-B): structure-function relationships. *Science.* 254:566–568.

Creuwels, L. A. J. M., L. M. G. v. Golde, and H. P. Haagsman. 1996. Surfactant protein B: effects on lipid domain formation and intermembrane lipid flow. *Biochim. Biophys. Acta.* 1285:1–8.

Cruz, A., C. Casals, and J. Perez-Gil. 1995. Conformational flexibility of pulmonary surfactant proteins SP-B and SP-C, studied in aqueous organic solvents. *Biochim. Biophys. Acta.* 1255:68–76.

Curstedt, T., H. Jörnvall, B. Robertson, T. Bergman, and P. Berggren. 1987. Two hydrophobic low-molecular-mass protein fractions of pulmonary surfactant: characterization and biophysical activity. *Eur. J. Biochem.* 168:255–262.

Curstedt, T., J. Johansson, J. Barros-Söderling, B. Robertson, G. Nilsson, M. Westberg, and H. Jörnvall. 1988. Low-molecular-mass surfactant protein type 1: the primary structure of a hydrophobic 8-kDa polypeptide with eight half-cystine residues. *Eur. J. Biochem.* 172:521–525.

Curstedt, T., J. Johansson, P. Persson, A. Eklund, B. Robertson, B. Löwenadler, and H. Jörnvall. 1990. Hydrophobic surfactant-associated polypeptides: SP-C is a lipopeptide with two palmitoylated cysteine residues, whereas SP-B lacks covalently linked fatty acyl groups. *Proc. Natl. Acad. Sci. USA.* 87:2984–2989.

Dobbs, L. G., J. R. Wright, S. Hawgood, R. Gonzales, K. Venstrom, and J. Nellenbogen. 1987. Pulmonary surfactant and its components inhibit secretion of phosphatidylcholine from cultured rat alveolar type II cells. *Proc. Natl. Acad. Sci. USA.* 84:1010–1014.

Galla, H.-J., N. Bourdos, A. von Nahmen, M. Amrein, and M. Sieber. 1998. The role of pulmonary surfactant protein C during the breathing cycle. *Thin Solid Films.* 327–329:632–635.

Glasser, S. W., T. R. Korfhagen, T. Weaver, T. Pilot-Matias, J. L. Fox, and J. A. Whitsett. 1987. cDNA and deduced amino acid sequence of human pulmonary surfactant-associated proteolipid SPL (Phe). *Proc. Natl. Acad. Sci. USA.* 84:4007–4011.

Goerke, J. 1974. Lung surfactant. *Biochim. Biophys. Acta.* 344:241–261.

Gotsmann, B., C. Seidel, B. Anczykowski, and H. Fuchs. 1999. Conservative and dissipative tip-sample interaction forces probed with dynamic AFM. *Phys. Rev. B.* 60:11051–11061.

Hatzis, D., G. Deiter, D. E. deMello, and J. Floros. 1994. Human surfactant protein-C: genetic homogeneity and expression in RDS; comparison with other species. *Exp. Lung Res.* 20:57–72.

Hawgood, S., B. Benson, J. Schilling, D. Damm, J. Clements, and R. White. 1987. Nucleotide and amino acid sequence of pulmonary surfactant protein SP 18 and evidence for cooperation between SP 18 and SP 28–36 in surfactant lipid adsorption. *Proc. Natl. Acad. Sci. USA.* 84: 66–70.

Hawgood, S. 1989. Pulmonary surfactant apoproteins: a review of protein and genomic structure. *Am. J. Physiol.* 257:L13–L22.

Jourdan, J. S., S. J. Cruchon-Dupeyrat, Y. Huan, P. K. Kuo, and G. Y. Lin. 1999. Imaging nanoscopic elasticity of thin film materials by atomic force microscopy: effects of force modulation frequency and amplitude. *Langmuir.* 15:6495–6504.

Kuroki, Y., R. J. Mason, and D. R. Voelker. 1988. Alveolar type II cells express a high-affinity receptor for pulmonary surfactant protein A. *Am. J. Respir. Cell Mol. Biol.* 8:5566–5570.

Lee, K. Y. C., M. M. Lipp, J. A. Zasadzinski, and A. J. Waring. 1998. Direct observation of phase and morphology changes induced by lung surfactant protein SP-B in lipid monolayers via fluorescence, polarized fluorescence, Brewster angle and atomic force microscopies. *SPIE.* 3273:115–133.

Lee, K. Y. C., M. M. Lipp, J. A. Zasadzinski, and A. J. Waring. 1997. Effects of lung surfactant specific protein SP-B and model SP-B peptide on lipid monolayers at the air-water interface. *Coll. Surf. A.* 128: 225–242.

Leufgen, K. M., H. Rulle, A. Benninghoven, M. Sieber, and H.-J. Galla. 1996. Imaging time-of-flight secondary-ion-mass spectrometry (TOF-SIMS) allows to visualize and analyze coexisting phases in Langmuir-Blodgett films. *Langmuir.* 12:1708–1711.

Lipp, M. M., K. Y. C. Lee, D. Y. Takamoto, J. A. Zasadzinski, and A. J. Waring. 1998. Coexistence of buckled and flat monolayers. *Phys. Rev. Lett.* 81:1650–1653.

Lipp, M. M., K. Y. C. Lee, J. A. Zasadzinski, and A. J. Waring. 1996. Phase and morphology changes in lipid monolayers induced by SP-B protein and its amino-terminal peptide. *Science.* 273:1196–1199.

Lipp, M. M., K. Y. C. Lee, W. A., and J. A. Zasadzinski. 1997. Fluorescence, polarized fluorescence, and Brewster angle microscopy of palmitic acid and lung surfactant protein B monolayers. *Biophys. J.* 72:1–21.

Magnov, S. N., V. Elings, and M.-H. Whangbo. 1997. Phase imaging and stiffness in tapping-mode atomic force microscopy. *Science.* 375: 2385–2391.

Miyamura, K., L. E. A. Leigh, J. Lu, J. Hopkins, A. Lopez-Bernal, and K. B. M. Reid. 1994. Surfactant protein D binding to alveolar macrophages. *Biochem. J.* 300:237–242.

Nogee, L. M., D. E. DeMello, L. P. Dehner, and H. R. Colten. 1993. Deficiency of pulmonary surfactant protein B in congenital alveolar proteinosis. *N. Engl. J. Med.* 328:406–410.

Olafson, R. W., U. Rink, S. Kielland, S.-H. Yu, J. Chung, P. G. R. Harding, and F. Possmayer. 1987. Protein sequence analysis studies on the low molecular weight hydrophobic proteins associated with bovine pulmonary surfactant. *Biochem. Biophys. Res. Comm.* 148:1406–1411.

Oosterlaken-Dijksterhuis, M. A., H. P. Haagsman, L. M. G. v. Golde, and R. A. Demel. 1991a. Interaction of lipid vesicles with monomolecular layers containing lung surfactant proteins SP-B or SP-C. *Biochemistry.* 30:8276–8281.

Oosterlaken-Dijksterhuis, M. A., H. P. Haagsman, L. M. G. v. Golde, and R. A. Demel. 1991b. Characterization of lipid insertion into monomolecular layers mediated by lung surfactant proteins SP-B and SP-C. *Biochemistry.* 30:10965–10971.

Pastrana-Rios, B., C. R. Flach, J. W. Brauner, A. J. Mautone, and R. Mendelsohn. 1994. A direct test of the "squeeze-out" hypothesis of lung surfactant function: external reflection FT-IR at the air/water interface. *Biochemistry.* 33:5121–5127.

Pastrana-Rios, B., S. Taneva, K. M. W. Keough, A. J. Mautone, and R. Mendelsohn. 1995. External reflection absorption infrared spectroscopy study of lung surfactant protein SP-B and SP-C in phospholipid monolayers at the air/water interface. *Biophys. J.* 69:2531–2540.

Pérez-Gil, J., C. Casals, and D. Marsh. 1995. Interactions of hydrophobic lung surfactant proteins SP-B and SP-C with dipalmitoylphosphatidylcholine and dipalmitoylphosphatidylglycerol bilayers studied by electron spin resonance spectroscopy. *Biochemistry.* 34:3964–3971.

Pérez-Gil, J., K. Nag, S. Taneva, and K. M. W. Keough. 1992. Pulmonary surfactant protein SP-C causes packing rearrangements of dipalmitoylphosphatidylcholine in spread monolayers. *Biophys. J.* 63:197–204.

Possmayer, F. 1988. A proposed nomenclature for pulmonary surfactant-associated proteins. *Am. Rev. Respir. Dis.* 138:990–998.

Possmayer, F., S.-H. Yu, J. M. Weber, and P. G. R. Harding. 1984. Pulmonary surfactant. *Can. J. Biochem. Cell Biol.* 62:1121–1133.

Post, A., A. von Nahmen, M. Schmitt, J. Ruths, H. Riegler, M. Sieber, and H.-J. Galla. 1995. Pulmonary surfactant protein C containing lipid films at the air-water interface as a model for the surface of lung alveoli. *Mol. Membr. Biol.* 12:93–99.

Rice, W. R., G. F. Ross, F. M. Singleton, S. Dingle, and J. A. Whitsett. 1987. Surfactant-associated protein inhibits phospholipid secretion from type II cells. *J. Appl. Physiol.* 63:692–698.

Shiffer, K., S. Hawgood, H. K. Haagsman, B. Benson, J. A. Clements, and J. Goerke. 1993. Lung surfactant proteins, SP-B and SP-C, alter the thermodynamic properties of phospholipid membranes: a differential calorimetric study. *Biochemistry.* 32:590–597.

Simatos, G. A., K. B. Forward, M. R. Morrow, and K. M. W. Keough. 1990. Interaction between perdeuterated dimyristoylphosphatidylcholine and low molecular weight pulmonary surfactant protein SP-C. *Biochemistry.* 29:5807–5814.

Suzuki, Y., Y. Fujita, and K. Kogishi. 1989. Reconstitution of tubular myelin from synthetic lipids and proteins associated with pig pulmonary surfactant. *Am. Rev. Respir. Dis.* 140:75–81.

Takahashi, A., and T. Fujiwara. 1986. Proteolipid in bovine lung surfactant: its role in surfactant. *Biochem. Biophys. Res. Comm.* 135: 527–532.

Taneva, S., and K. M. W. Keough. 1994. Pulmonary surfactant proteins SP-B and SP-C in spread monolayers at the air-water interface. I. Monolayers of pulmonary surfactant protein SP-B and phospholipids. *Biophys. J.* 66:1137–1148.

Tenner, A. J., S. L. Robinson, J. Borchelt, and J. R. Wright. 1989. Human pulmonary surfactant protein (SP-A), a protein structurally homologous to C1q, can enhance FcR- and CR1-mediated phagocytosis. *J. Biol. Chem.* 264:13923–13928.

van Iwaarden, F. v., B. Welmers, J. Verhoef, H. P. Haagsman, and L. M. G. v. Golde. 1990. Pulmonary surfactant protein A enhances the host-defense mechanism of rat alveolar macrophages. *Am. J. Res. Cell Mol. Biol.* 2:91–98.

Vandenbussche, G., A. Clercx, M. Clercx, T. Curstedt, J. Johansson, H. Jörnvall, and J.-M. Ruysschaert. 1992. Secondary structure and orientation of the surfactant protein SP-B in a lipid environment: a Fourier transform infrared spectroscopy study. *Biochemistry.* 31:9169–9176.

Vincent, J. S., S. D. Revak, C. D. Cochrane, and I. W. Levin. 1993. Interactions of model human pulmonary surfactants with a mixed phospholipid bilayer assembly: Raman spectroscopic studies. *Biochemistry.* 32:8228–8238.

von Nahmen, A., A. Post, H.-J. Galla, and M. Sieber. 1997a. The phase behavior of lipid monolayers containing pulmonary surfactant protein C studied by fluorescence light microscopy. *Eur. Biophys. J.* 26:359–369.

von Nahmen, A., M. Schenk, M. Sieber, and M. Amrein. 1997b. The structure of a model pulmonary surfactant as revealed by scanning force microscopy. *Biophys. J.* 72:463–469.

Voorhout, W. F., T. Veenendaal, H. P. Haagsman, A. J. Verkleij, L. M. G. van Golde, and H. J. Geuze. 1991. Surfactant protein A is localized at the corners of the pulmonary tubular myelin lattice. *J. Histochem. Cytochem.* 39:1331–1336.

Vorbroker, D. K., S. A. Profitt, L. A. Nogee, and J. A. Whitsett. 1995. Aberrant processing of surfactant protein C in hereditary SP-B deficiency. *Am. J. Physiol.* 268:L647–L656.

Williams, M. C., S. Hawgood, and R. L. Hamilton. 1991. Changes in lipid structure produced by surfactant proteins SP-A, SP-B, and SP-C. *Am. J. Res. Cell Mol. Biol.* 5:41–50.

Wright, J. R., R. E. Wager, S. Hawgood, L. Dobbs, and J. A. Clements. 1987. Surfactant apoprotein M_r = 26,000–36,000 enhances uptake of liposomes by type II cells. *J. Biol. Chem.* 262:2888–2894.

Yu, S.-H., and F. Possmayer. 1992. Effect of pulmonary surfactant protein B (SP-B) and calcium on phospholipid adsorption and squeeze-out of phosphatidylglycerol from binary phospholipid monolayers containing dipalmitoylphosphatidylcholine. *Biochim. Biophys. Acta.* 1126:26–34.